Output-only modal parameter identification of systems subjected to various type excitations

Eimantas Poskus[1], Geoffrey W. Rodgers[2], and J. Geoffrey Chase[3]

[1]Department of Mechanical Engineering, University of Canterbury, Private Bag 4800, Christchurch 8140, New Zealand, Corresponding author, Email: eimantasposkus@gmail.com

[2]Department of Mechanical Engineering, University of Canterbury, Private Bag 4800, Christchurch 8140, New Zealand, Email: geoff.rodgers@canterbury.ac.nz

[3]Department of Mechanical Engineering, University of Canterbury, Private Bag 4800, Christchurch 8140, New Zealand, Email: geoff.chase@canterbury.ac.nz

ABSTRACT

This study presents a novel modal parameter identification method enabling approximation of the mode shapes of linear systems using white noise or earthquake inputs. The majority of well established existing system identification methods perform successfully when the system is excited by broadband white noise excitation. However, they encounter serious limitations when analysing the vibrations triggered by non-stationary earthquake inputs. Thus, the presented technique extends the applicability of system identification and modal based structural health monitoring methods. The method operates in modal space and is based on mode superposition in short windows. The mode shapes are identified using an optimization algorithm minimizing the weighted sum of cross-correlation of frequency response spectra. The technique is validated analytically using simulation results of a simple 3D structure representing a simplified model of a real bridge pier structure, which enables exact comparison to known properties. The results show the method provides relatively good identification accuracy of modal parameters of systems excited by white noise and earthquake inputs. The identified modal frequencies showed <1% error, where the mode shape coefficients

were identified within 5% error. The method performs robustly even for high levels of simulated sensor noise and can be readily applied to more complex MDOF systems.

Keywords: modal parameters, output-only modal identification, structural health monitoring

INTRODUCTION

A number of different structural health monitoring (SHM) methods have been developed to identify damage. Many are vibration-based SHM methods developed to capture changes in modal parameters (Brownjohn et al. 2010; Astroza et al. 2013; Astroza et al. 2016a; Astroza et al. 2016b; Moaveni et al. 2010; Nagarajaiah and Basu 2009; Saaed and Nikolakopoulos 2016) . These changes can be represented as a damage index (Doebling et al. 1996; Amezquita-Sanchez and Adeli 2015; Singhal and Kiremidjian 1996; Ren and De Roeck 2002) or used for reconstruction of second order models (Luş et al. 2002; Luş et al. 2004; Hong et al. 2009). They are popular because of their use with measured, small ambient vibrations to identify linear responses and systems.

The eigensystem realization algorithm (ERA) (Juang and Pappa 1985) and its combination with natural excitation techniques (NExT/ERA) (Moaveni et al. 2008; Pappa et al. 1998; Moncayo et al. 2010; Caicedo 2011) or the Observer/Kalman Filter Identification (OKID) (Juang et al. 1993; Vicario et al. 2015; Fraraccio et al. 2008) are two of the more commonly used modal parameter identification techniques for linear time-invariant systems subjected to white noise excitations. A number of studies (Astroza et al. 2016a; Moaveni et al. 2010; Brownjohn et al. 2010) used a stochastic subspace identification (SSI) technique (Vicario et al. 2015) to identify modal parameters of simulated and real life structures. Successful SHM in these conditions has also been implemented using different variations of autoregressive moving average (ARMA) (Carden and Brownjohn 2008; Bodeux and Golinval 2001; da Silva et al. 2008; Sohn and Farrar 2001) and enhanced frequency domain decomposition (EFDD) methods (Brincker et al. 2001; Jacobsen et al. 2008; Moaveni et al. 2010; Astroza et al. 2016a).

All these techniques are limited to linear time-invariant systems. Moreover, most perform best when the input loads meet specific characteristics, such as broad band white noise, which is not a typical condition. The ability to easily use ambient vibrations without constraint or knowledge of the input would be more ideal for regular monitoring, requiring an output-only SHM method.

This research presents a new modal parameter identification technique based on mode decomposition to perform as an output only identification technique for linear time-invariant systems using relatively long duration response measurements extracted from ambient load or even larger, shorter duration earthquake induced vibrations. The method is not limited to any characteristics of the input load. In addition, for longer, non-linear seismic responses these parameters can be identified within short windows over the event. Finally, the approximated constant mode shapes can be used to decompose the modes, which can be used for reconstruction of single mode dominant hysteresis loops that can be readily analysed for changes or damage using hysteresis loop analysis (HLA) (Zhou et al. 2015; Zhou et al. 2017).

METHOD

Mode decoupling

The equation of motion of a linear multi-degree-of-freedom (MDOF) system is described:

$$\mathbf{M}\{\ddot{X}\} + \mathbf{C}\{\dot{X}\} + \mathbf{K}\{X\} = \mathbf{M}r\{\ddot{X}_g\} \tag{1}$$

where $\mathbf{M}$, $\mathbf{C}$, $\mathbf{K}$ are the mass, damping and stiffness matrices, r is the excitation influence vector, $\{\ddot{X}\}$, $\{\dot{X}\}$ and $\{X\}$ are the acceleration, velocity and displacement vectors of MDOF system, respectively, and $\{\ddot{X}_g\}$ is the ground motion acceleration.

Assuming the modes shapes are real-valued, the linear MDOF system response can be represented as the weighted, linear sum of individual vibration modes:

$$X(t) = \sum_{i=1}^{n} \phi_i \cdot \overline{x}_i(t) = \Phi\overline{X}(t) = \begin{bmatrix} \phi_{1,1} \cdot \overline{x}_1(t) + \cdots + \phi_{1,n} \cdot \overline{x}_n(t) \\ \vdots \\ \phi_{n,1} \cdot \overline{x}_1(t) + \cdots + \phi_{n,n} \cdot \overline{x}_n(t) \end{bmatrix} \tag{2}$$

where n is the number of modes, $\overline{X}(t) = \begin{bmatrix}\overline{x}_1(t) & \overline{x}_2(t) & \cdots & \overline{x}_n(t)\end{bmatrix}^T$ is modal displacement vector of n modes at time instant t, where each row of $\overline{X}(t)$ represents each mode, $\overline{x}_i(t)$, $\Phi = \begin{bmatrix}\phi_1 & \phi_2 \ldots \phi_i \ldots \phi_n\end{bmatrix}$ is the $n \times n$ mode shape matrix calculated by solving an eigenvalue problem, where ϕ_i is $n \times 1$ mode shape vector of the i^{th} mode.

In this study, a relatively simple tool is proposed to approximate $\hat{\Phi}$ using the principle of mode superposition. Although the method is limited to systems with real-valued modes, a number of studies (Moaveni et al. 2010; Moaveni et al. 2013; Astroza et al. 2016c) demonstrated that for civil structures the lowest modes are typically real or near real-valued. The modal response, $\overline{X}$, of a linear structure can be described, per Equation (2):

$$\overline{X} = \hat{\Phi}^{-1} X = \begin{bmatrix}\hat{\phi}_{1,1} & \cdots & \hat{\phi}_{1,n} \\ \vdots & \ddots & \vdots \\ \hat{\phi}_{n,1} & \cdots & \hat{\phi}_{n,n}\end{bmatrix}^{-1} \begin{bmatrix}\phi_{1,1} \cdot \overline{x}_1 + \cdots + \phi_{1,n} \cdot \overline{x}_n \\ \vdots \\ \phi_{n,1} \cdot \overline{x}_1 + \cdots + \phi_{n,n} \cdot \overline{x}_n\end{bmatrix} \tag{3}$$

where n is the number of DOFs, and $\hat{\Phi}$ is an approximate mode shape matrix, where ideally $\hat{\Phi} = \Phi$. The hat symbol here is used to denote identified/approximated parameters in this study.

In real structures, the exact number of modes contributing to the structure's response is often unknown and can be very large, as with suspension bridges (Farrar et al. 1996). For practical reasons only a limited number of DOFs are monitored, making full mode decomposition infeasible. However, partial decomposition can be carried out using limited DOFs, which is still practical for real structures, because higher modes often have negligible response energy. In addition, most civil structure design codes neglect the influence of higher modes, as they contribute less than 10% to the total effective modal mass (CEN 2004).

For a structure modelled with $m = 2$ DOFs of n total DOFs using Equation (2) for X, the estimated modal response $\overline{X}_{p,m}$, where p in the subscript refers to partial decoupling, can be written:

$$
\begin{aligned}
\overline{X}_{p,2} =& \hat{\Phi}^{-1} X = \begin{bmatrix} \hat{\phi}_{1,1} & \hat{\phi}_{1,2} \\ \hat{\phi}_{2,1} & \hat{\phi}_{2,2} \end{bmatrix}^{-1} \begin{bmatrix} \phi_{1,1} \cdot \overline{x}_1 + \phi_{1,2} \cdot \overline{x}_2 + \cdots + \phi_{1,n} \cdot \overline{x}_n \\ \phi_{2,1} \cdot \overline{x}_1 + \phi_{2,2} \cdot \overline{x}_2 + \cdots + \phi_{2,n} \cdot \overline{x}_n \end{bmatrix} = \\
&= \frac{1}{det(\hat{\Phi})} \left[\begin{matrix} (\hat{\phi}_{2,2} \cdot \phi_{1,1} - \hat{\phi}_{1,2} \cdot \phi_{2,1})\overline{x}_1 + (\hat{\phi}_{2,2} \cdot \phi_{1,2} - \hat{\phi}_{1,2} \cdot \phi_{2,2})\overline{x}_2 \\ (-\hat{\phi}_{2,1} \cdot \phi_{1,1} + \hat{\phi}_{1,1} \cdot \phi_{2,1})\overline{x}_1 + (-\hat{\phi}_{2,1} \cdot \phi_{1,2} + \hat{\phi}_{1,1} \cdot \phi_{2,2})\overline{x}_2 \end{matrix} \right. \\
&\quad \left. \begin{matrix} + \cdots + (\hat{\phi}_{2,2} \cdot \phi_{1,n} - \hat{\phi}_{1,2} \cdot \phi_{2,n})\overline{x}_n \\ + \cdots + (-\hat{\phi}_{2,1} \cdot \phi_{1,n} + \hat{\phi}_{1,1} \cdot \phi_{2,n})\overline{x}_n \end{matrix} \right]
\end{aligned} \tag{4}
$$

where $\phi_{j,i}$ and $\hat{\phi}_{j,i}$ represent the true and identified mode shape coefficients, respectively. If $\hat{\phi}_{j,i}$ can be identified exactly, then $\hat{\phi}_{1,1} = \phi_{1,1}$, $\hat{\phi}_{2,1} = \phi_{2,1}$, $\hat{\phi}_{1,2} = \phi_{1,2}$ and $\hat{\phi}_{2,2} = \phi_{2,2}$. From the assumed perfect identification, the result of the decomposition is defined:

$$
\begin{aligned}
\overline{X}_{p,2} &= \begin{bmatrix} 1 \cdot \overline{x}_1 + 0 \cdot \overline{x}_2 + \cdots + \frac{(\hat{\phi}_{2,2} \cdot \phi_{1,i} - \hat{\phi}_{1,2} \cdot \phi_{2,i})}{det(\hat{\Phi})}\overline{x}_i + \cdots + \frac{(\hat{\phi}_{2,2} \cdot \phi_{1,n} - \hat{\phi}_{1,2} \cdot \phi_{2,n})}{det(\hat{\Phi})}\overline{x}_n \\ 0 \cdot \overline{x}_1 + 1 \cdot \overline{x}_2 + \cdots + \frac{(-\hat{\phi}_{2,1} \cdot \phi_{1,i} + \hat{\phi}_{1,1} \cdot \phi_{2,i})}{det(\hat{\Phi})}\overline{x}_i + \cdots + \frac{(-\hat{\phi}_{2,1} \cdot \phi_{1,n} + \hat{\phi}_{1,1} \cdot \phi_{2,n})}{det(\hat{\Phi})}\overline{x}_n \end{bmatrix} = \\
&= \begin{bmatrix} 1 \cdot \overline{x}_1 + 0 \cdot \overline{x}_2 + \cdots + \alpha_{1,i} \cdot \overline{x}_i + \cdots + \alpha_{1,n} \cdot \overline{x}_n \\ 0 \cdot \overline{x}_1 + 1 \cdot \overline{x}_2 + \cdots + \alpha_{2,i} \cdot \overline{x}_i + \cdots + \alpha_{2,n} \cdot \overline{x}_n \end{bmatrix}
\end{aligned} \tag{5}
$$

where $\alpha_{1,i}$ and $\alpha_{2,i}$ are scaling factors that result for each mode.

More generally, for a system with m modeled DOFs of n total DOFs, the estimated modal response $\overline{X}_p$ can be written:

$$\overline{X}_{p,m} = \begin{bmatrix} 1 \cdot \overline{x}_1 + 0 \cdot \overline{x}_2 + \cdots + 0 \cdot \overline{x}_m + \alpha_{1,m+1}\overline{x}_{m+1} + \cdots + \alpha_{1,n}\overline{x}_n \\ 0 \cdot \overline{x}_1 + 1 \cdot \overline{x}_2 + \cdots + 0 \cdot \overline{x}_m + \alpha_{2,m+1}\overline{x}_{m+1} + \cdots + \alpha_{2,n}\overline{x}_n \\ \cdots \\ 0 \cdot \overline{x}_1 + 0 \cdot \overline{x}_2 + \cdots + 1 \cdot \overline{x}_m + \alpha_{m,m+1}\overline{x}_{m+1} + \cdots + \alpha_{m,n}\overline{x}_n \end{bmatrix} = \\ = \begin{bmatrix} 1 & 0 & \cdots & 0 & \alpha_{1,m+1} & \cdots & \alpha_{1,n} \\ 0 & 1 & \cdots & 0 & \alpha_{2,m+1} & \cdots & \alpha_{2,n} \\ \vdots & \vdots & \ddots & \vdots & \vdots & \ddots & \vdots \\ 0 & 0 & \cdots & 1 & \alpha_{m,m+1} & \cdots & \alpha_{m,n} \end{bmatrix} \overline{X} = A\overline{X} \tag{6}$$

where $\alpha_{m,n}$ is the n^{th} mode scaling factor and A is a mode scaling matrix defining contribution of omitted modes, $m+1 \ldots n$. Thus, the i^{th} modal response will consist of the i^{th} mode itself and scaled modes that are omitted by a perfectly approximated ($\hat{\Phi} = \Phi$) mode shape matrix ($\hat{\Phi}$). The contribution of other modes is thus, ideally, equal to zero.

It can also be shown for the approximated mode shape matrix, $\hat{\Phi}$, where modal coefficients are optimized only for the i^{th} mode (with a goal $\hat{\phi}_i = \phi_i$) using Equation (3), the following mode decomposition and mode scaling matrix, A, is obtained:

$$\overline{X}_{p,m} = \hat{\Phi}^{-1} X = \begin{bmatrix} \alpha_{1,1} & \alpha_{1,2} & \cdots & 0 & \cdots & \alpha_{1,n} \\ \alpha_{2,1} & \alpha_{2,2} & \cdots & 0 & \cdots & \alpha_{2,n} \\ \cdots & \cdots & \cdots & \cdots & \cdots & \cdots \\ \alpha_{i,1} & \alpha_{i,2} & \cdots & 1 & \cdots & \alpha_{i,n} \\ \cdots & \cdots & \cdots & \cdots & \cdots & \cdots \\ \alpha_{m,1} & \alpha_{m,2} & \cdots & 0 & \cdots & \alpha_{m,n} \end{bmatrix} \begin{bmatrix} \overline{x}_1 \\ \overline{x}_2 \\ \cdots \\ \overline{x}_i \\ \cdots \\ \overline{x}_n \end{bmatrix} \tag{7}$$

Thus, the modal response of the i^{th} mode, $\overline{x}_i$, is removed from the modal responses of all other modes due to the zeros in the i^{th} column. This result means the full/partial decomposition per Equation (6) can be achieved by approximating each mode shape individually, thus applying mode-by-mode identification.

Estimating cross-correlation of frequency response spectra

Mode contribution/coupling can be quantified by calculating its energy content in the frequency domain. Ideally, the i^{th} mode would have very small spectral energy in the other modes if $\hat{\phi}_i$ is perfectly identified as in Equation (7). Assuming the absolute acceleration is monitored, thus $\ddot{X}^{abs} = \ddot{X} - r\ddot{X}_g$, the decomposed modal absolute acceleration, $\overline{\ddot{X}}$, can be represented in the frequency domain by carrying out an FFT analysis:

$$\overline{Y}(\hat{\Phi}) = \left|FFT(\overline{\ddot{X}}_{p,m})\right| = \left|\overline{\ddot{X}}_{p,m} W_{FFT}\right| = \left|\hat{\Phi}^{-1}\ddot{X}^{abs} W_{FFT}\right| \tag{8}$$

where W_{FFT} is the Fourier transformation matrix defined, $W_{FFT}(n,k) = W_N^{(n-1)(k-1)}$, where $W_N = e^{(-2\pi i)/N}$, $(n = 1 \ldots N)$, N is the discrete length of the monitored signal X, and $k = 1 \ldots K$, where K is the number of frequency bins in the analysis.

As a result $\overline{Y}(\hat{\Phi}) = \begin{bmatrix} \overline{y}_1 & \overline{y}_2 & \cdots & \overline{y}_m \end{bmatrix}^T$ is $m \times K$, where each row of $\overline{Y}(\hat{\Phi})$ represents the frequency response spectrum (FRS) of each mode. In the case of perfect identification, $\hat{\Phi} = \Phi$, the FRS of each mode, $\overline{y}_i$, will represent a Single-Degree-of-Freedom (SDOF) linear time-invariant (LTI) mechanical system, which for the i^{th} mode response can be described:

$$\overline{y}_i(\omega) = \overline{F}(\omega) \cdot H_i(\omega) \tag{9}$$

where $\overline{F}(\omega)$ is the Fourier transform of an input and $H_i(\omega)$ is the frequency response function for the i^{th} mode.

For perfect identification, $\hat{\phi}_i = \phi_i$ per Equation (7), the i^{th} mode response will have zero contribution from other modes. This contribution can be quantified in the frequency domain by calculating the cross-correlation of the i^{th} mode's frequency response spectrum with respect to the frequency response spectrum of the other modes and expressed as a function of the i^{th} mode shape, $\hat{\phi}_i$, yielding:

$$corr^{iso,i}(\hat{\phi}_i) = \overline{y}_i^{n,iso}(\hat{\phi}_i)\overline{Y}^n(\hat{\phi}_i)^T \tag{10}$$

where the term n in the superscript refers to the normalized FRS, $\overline{y}_i^n \cdot \overline{y}_i^{nT} = 1$, $\overline{y}_i^{n,iso}$ is the normalized FRS of the i^{th} mode isolated around the natural frequency, ω_i:

$$\overline{y}_i^{iso}(\hat{\Phi}) = \overline{y}_i(\hat{\Phi})\mathrm{diag}(N_i) \tag{11}$$

where N_i is a $K \times 1$ shape vector used to segregate a given mode's FRS to calculate its energy without other modes contributing, where K, again, is the number of frequency bins used for FFT analysis as defined in Equation (8). The term $diag$ refers to transformation of a column vector into a diagonal matrix. Shape vector, N, can be formulated using any windowing function, as shown in Figure 1.

In this study, a peak segregation function, N_i, is formulated using a Hanning windowing technique. Effective window length is taken as a factor of the estimated frequency bandwidth, $\Delta\omega$, determined from the fitted FRF, $\hat{H}_i(\omega)$, (from Equation (9)) at the response level of $\left|\hat{H}_i\right|/\sqrt{2}$ as shown in Figure 1. Hence, the shape function can be written:

$$\begin{aligned} N_i(\omega) &= 0 && \omega < \omega_i - \frac{W}{2}\cdot\Delta\omega \\ &= 0.5\cdot\left(1-\cos\left(2\pi\frac{n}{N}\right)\right) && \omega_i - \frac{W}{2}\cdot\Delta\omega \le \omega \le \omega_i + \frac{W}{2}\cdot\Delta\omega \\ &= 0 && \omega > \omega_i + \frac{W}{2}\cdot\Delta\omega \end{aligned} \tag{12}$$

where $n = \omega - (\omega_i - \frac{W}{2}\cdot\omega)$, $N = W\cdot\Delta\omega$ where $\Delta\omega$ is the frequency bandwidth at the response level of $\left|\hat{H}_i\right|/\sqrt{2}$, and W is the assumed effective peak isolation width.

Thus, the mode segregation function, N_i, is re-evaluated for each time window after FRF least-square fitting is performed. This approach enables identification of time-varying systems. Window segments may be continuous or partially overlapping depending on the resolution of time-varying parameter changes desired. However, it should be noted that windowing function, N_i, is only used to estimate cross correlation between windowed FRS of i^{th} mode, $\overline{y}_i^{iso}$, and the other mode FRS, $\overline{Y}$.

Optimizing mode shape coefficients

The efficiency of the partial decoupling for mode i can thus be estimated by summing all the weighted correlation coefficients ($j = 1..m$, $j \neq i$), excluding correlation of the mode with itself:

$$Corr^{iso,i}(\hat{\phi}_i) = \sum_{j=1, j\neq i}^{m} w_j^i \cdot corr_j^{iso,i}(\hat{\phi}_i) \tag{13}$$

where w_j^i is the weighting coefficient that enforces mode orthogonality or scales the correlation coefficients based on Modal Assurance Criteria (MAC) (Allemang 2003):

$$\begin{aligned} w_j^i &= \left(1 + \frac{\sqrt{MAC_{i,j}} + \sqrt{MAC_{i,j}^{mirr}}}{2}\right)^2 \\ MAC_{i,j} &= \frac{\left|\hat{\phi}_i^{\,T} \hat{M} \hat{\phi}_j\right|^2}{\left(\hat{\phi}_i^{\,T} \hat{M} \hat{\phi}_i\right) \cdot \left(\hat{\phi}_j^{\,T} \hat{M} \hat{\phi}_j\right)} \\ MAC_{i,j}^{mirr} &= \frac{\left|\left(\hat{\phi}_i^{\,mirr}\right)^T \hat{M} \hat{\phi}_j\right|^2}{\left(\left(\hat{\phi}_i^{\,mirr}\right)^T \hat{M} \hat{\phi}_i^{\,mirr}\right) \cdot \left(\hat{\phi}_j^{\,T} \hat{M} \hat{\phi}_j\right)} \end{aligned} \tag{14}$$

where $\hat{M}$, is the assumed/approximated mass matrix of the system, which acts as a scaling matrix.

If no priori knowledge is known about the structure to estimate this mass, an identity matrix can be taken. $MAC_{i,j}$ is the modal assurance criteria coefficient expressing the degree of consistency or orthogonality between the optimized i^{th} modal vector, $\hat{\phi}_i$, and the other estimated mode shape coefficients, $\hat{\phi}_{j=1...m}$. $MAC_{i,j}^{mirr}$ is the coefficient expressing the degree of similarity between optimized mirrored mode shape, $\hat{\phi}_i^{\,mirr}$, and all other estimated mode shape coefficients, $\hat{\phi}_{j=1...m}$. The mirrored mode shape vector, $\hat{\phi}_i^{\,mirr}$ is the mode shape vector $\hat{\phi}_i$ mirrored around either of the principal axes, x or y:

$$\hat{\phi}_i^{mirr} = \hat{\phi}_i^{mirr,x} = \begin{bmatrix} \hat{\phi}_{i,x} \\ -\hat{\phi}_{i,y} \end{bmatrix} \quad \text{or} \quad \hat{\phi}_i^{mirr} = \hat{\phi}_i^{mirr,y} = \begin{bmatrix} -\hat{\phi}_{i,x} \\ \hat{\phi}_{i,y} \end{bmatrix} \tag{15}$$

where $\hat{\phi}_{i,x}$ and $\hat{\phi}_{i,y}$ are the i^{th} mode shape vector components in x and y direction, respectively. Thus, the correlation scaling factor provided in Equation (14) will enforce mode shape optimization orthogonalized around the principal axes in case of overlapping or very closely spaces modes.

Finally, the solution to the optimal i^{th} mode shape coefficients can be written as the solution to the following optimization problem:

$$(\hat{\phi}_i) = \arg\min_{\hat{\phi}_i}(Corr^{iso,i}(\hat{\phi}_i)) \tag{16}$$

Once the optimal approximated mode shape coefficients $\hat{\phi}_i$ for mode i are found, the optimization can proceed for the next mode, as shown in Figure 2.

When mode-by-mode identification is carried out, detection of new modal frequencies or poles becomes an easy task because the modes with high spectral energy are already removed from the FRS of unidentified modes due to the zeros in Equation (7). The optimization problem can be readily solved using the unconstrained non-linear multivariable solver available in MATLAB. A more detailed version of the mode identification routine is shown in the flow chart of Figure 3.

Modified Gram-Schmidt orthogonalization

As the mode shape coefficients go through the optimization process of Equation (16), it is important to ensure mode orthogonality with respect to the other modes, to allow the solver to converge optimal values. Mode orthogonality can be obtained using the modified Gram-Schmidt orthogonalization process, which generates a set of mode shape coefficients that is orthogonal to all the subsequent mode shapes. The j^{th} mode shape can be mass orthogonalized with respect to the i^{th} mode (Chopra 1995):

$$\hat{\phi}_j^{orth} = \hat{\phi}_j - \hat{\phi}_i \cdot \frac{\hat{\phi}_j^T \hat{M} \hat{\phi}_i}{\hat{\phi}_i^T \hat{M} \hat{\phi}_i} \tag{17}$$

where $\hat{M}$ is the assumed/approximated mass matrix. If no *a-priori* knowledge about the structure is known, an identity matrix can be used.

Mode orthogonalization can be implemented as a part of the objective function, or as an additional step, which would then require an additional convergence loop. Although the mode shape optimization is carried out for the i^{th} mode, meaning only the $\hat{\phi}_i^{orth}$ terms are being varied, in fact due to the orthogonalization process of Equation (17), all the terms of $\hat{\Phi}^{orth}$ are being varied in the optimization loop, as shown in flowchart of Figure 3. However, after each optimization iteration, only the i^{th} mode and the rest of unidentified modes will be updated, as defined in Step 8 of Figure 3. This approach ensures previously identified modes are not being altered.

Damping and frequency estimation

A successful mode shape identification decomposes the response into separate modes. In the frequency domain, this outcome results in a set of single transfer functions, each representing SDOF system without any residuals from adjacent modes, per Equation (6). However, in real life situations, structures often have an infinitely large number of difficult to identify modes with very low energy. As a result, the modal transfer functions will often contain some contribution from residuals due to unidentified or poorly identified modes (Ewins 2000).

Assuming the contribution from the other modes is negligible, the frequency response spectrum, $\overline{y}_i(\omega)$, of i^{th} mode can be approximated, per Equation (9):

$$\hat{\overline{y}}_i(\omega) = \hat{H}_i(\omega) \cdot \overline{F}(\omega) = \frac{Q_i}{\hat{\omega}_i^2 - \omega^2 + 2i\hat{\xi}\omega\hat{\omega}_i} \cdot \overline{F}(\omega) \tag{18}$$

where $\hat{H}_i(\omega)$ is the fitted FRF function for mode i, $\hat{\omega}_i$ is the identified natural frequency and $\hat{\xi}_i$ is the identified modal damping ratio. Thus, the modal parameters ($\hat{\omega}_i$ and $\hat{\xi}_i$) can be identified using curve fitting methods (Jacobsen et al. 2008) assuming the modal parameters do not vary throughout the analyzed time window and assuming the input excitation, $\overline{F}(\omega)$, is known or is constant in case of broadband white noise excitation, $\overline{F}(\omega) = const$. In this study a least-square-fit is utilized to minimize the error between the approximated, $\hat{\overline{y}}_i$, and calculated, $\overline{y}_i$, FRS across the range of modal coordinates.

Mode identification process summary

Initial modal parameter identification

The initial mode shape identification, when no prior knowledge about the structure is known, can be described as a step process and is shown in the flowchart of Figure 3:

Step 1. Analysis initialization: Choose the time segment, collect $m \times s$ data matrix, $X = \begin{bmatrix} x_1 & x_2 & \cdots & x_m \end{bmatrix}^T$, where m is the number of measured DOFs and $s = (t_1 - t_0) \cdot f_s$ is the number of samples, t_0 is the start and t_1 the end of the time window, and f_s is the sampling frequency. Assign a random orthogonal mode shape matrix, $\hat{\Phi}^{init}$, where *init* refers to initial identification guess. Initialize mode number $i = 1$.

Step 2. Selecting the strongest mode: Transform the data into the modal space using Equation (3), and obtain the FRS of each modal response, $\overline{Y}(\hat{\Phi}^{init}) = \begin{bmatrix} \overline{y}_1 & \overline{y}_2 & \cdots & \overline{y}_m \end{bmatrix}^T$, by transforming it into the frequency domain using Equation (8). Analyse all FRS for unidentified modes, (from i to m modes), and find the mode, $\overline{y}_{e_{max}}$, with the strongest energy, where e_{max} is the mode index number. Rearrange the approximated mode shape matrix, $\hat{\Phi}^{init}\,(:, [i\ e_{max}]) = \hat{\Phi}^{init}\,(:, [e_{max}\ i])$ and redo the transformation for $\overline{Y}(\hat{\Phi}^{init})$ using Equation (8).

Step 3. Mode/ peak identification: Identify the modal frequency with the strongest energy from the i^{th} modes's FRS, $\overline{y}_i^{abs}(\omega)$, and create shape function, N_i^{mode}, using Equation (12) for the i^{th} mode, which will segregate the FRS around the selected modal frequency. Calculate the isolated FRS for mode i, $\overline{y}_i^{iso}(\hat{\Phi}^{init})$ using Equation (11). Use Equations (10) and (13) to calculate the initial correlation coefficient $R_{iter=0} = Corr^{iso,i}\left(\hat{\phi}_i^{init}\right)$.

Step 4. Setting up an optimization problem / objective function: Create optimization matrix, $\hat{\Phi}^{orth} = \hat{\Phi}^k$. Define the optimization matrix i^{th} column as a function of $\hat{\phi}_i^{orth} = \left[\hat{\phi}_{1,i}^{orth} \quad \hat{\phi}_{2,i}^{orth} \quad \cdots \quad \hat{\phi}_{m,i}^{orth}\right]^T$. Mode shape coefficients for the other modes will be subjected to Gram-Schmidt orthogonalization. Define the correlation coefficient, calculated per Equation (13), as a function of $\hat{\phi}_i^{orth} = \left[\hat{\phi}_{1,i}^{orth} \quad \hat{\phi}_{2,i}^{orth} \quad \cdots \quad \hat{\phi}_{m,i}^{orth}\right]^T$:

$$Corr^{iso,i}\left(\hat{\phi}_i^{orth}\right) = Corr^{iso,i}\left(\left[\hat{\phi}_{1,i}^{orth} \quad \hat{\phi}_{2,i}^{orth} \quad \cdots \quad \hat{\phi}_{m,i}^{orth}\right]^T\right)$$

Step 5. Solving optimization problem: Solve linear unconstrained optimization problem using Equation (16) and obtain the optimized mode shape coefficients for the i^{th} mode, $\hat{\phi}_i^{orth}$.

Step 6. Performing orthogonalization: Orthogonalize all mode shape coefficients with respect to identified mode shape coefficients, $\hat{\phi}_i^{orth}$, using the modified Gram-Schmidt method, of Equation (17). Mode orthogonalization can be implemented inside the objective function or after optimization, by creating an additional convergence loop.

Step 7. Checking the convergence: Calculate the total correlation coefficient, $R_{iter} = Corr^{iso,i}\left(\hat{\phi}_i^{init}\right)$ per Equation (13), and check the convergence:

$$Conv_{iter} = \frac{R_{iter-1} - R_{iter}}{R_{iter-1}} \tag{19}$$

Step 8. Updating the mode shape matrix: Update the approximated mode shape matrix's i^{th} mode shape and the rest of unidentified modes (uidm) $\hat{\Phi}^{init}$(:, [i uidm]) = $\hat{\Phi}^{orth}$(:, [i uidm]). If the convergence value is greater than $Conv_{iter} > 1e^{-6}$, return to **Step 4**.

Step 9. Mode shape verification: Verify the newly identified mode by evaluating it's FRS. In case of successful identification, the pole will be clearly visible, whereas the same peak will be removed from other mode's FRS, $\overline{y}_i(\hat{\Phi}^{init})$, or in other words the rest of the modes will contain no residuals from the newly identified mode, which acts as a noise. This result means if the whole identification loop process is re-iterated from **Step 3**, by setting $i = 1$, thus starting from mode 1, the identification will yield more accurate mode shapes.

Step 10. Stepping back to look for new modes / poles: Step to the next mode, $i = i + 1$, and return to **Step 2**.

METHOD VALIDATION AND ANALYSES

Test structure

The proposed method is validated analytically using a 3D FE model representing a simplified model of a bridge pier structure shown in Figure 4. It is a $7.3m$ long circular $1.2m$ diameter reinforced concrete column rigidly connected to the footing. Concrete blocks are attached to the top of the cantilever column, which represents the mass of the bridge deck. The structure is simplified into a 4 degrees-of-freedom (DOF) system, with 2 DOFs in each direction, as shown in Figure 4. More details on the test structure are provided in (Schoettler et al. 2012). The estimated effective second moment of area around both axis is $I_x = I_y = 0.1m^4$, the modulus of elasticity of the concrete is $E = 22.9GPa$.

The estimated translational mass in x and y directions is $M_x = M_y = 2.7 \cdot 10^5 kg$, whereas the rotational masses around x and y directions are different resulting in $M_{\phi_x} = 0.68 \cdot 10^6 kg$ and $M_{\phi_y} = 1.16 \cdot 10^6 kg$. The following stiffness matrix and diagonal mass matrix are obtained for a linear 4 DOF system:

$$K = \begin{bmatrix} 0.088 & 0.322 & 0 & 0 \\ 0.322 & 1.565 & 0 & 0 \\ 0 & 0 & 0.088 & -0.322 \\ 0 & 0 & -0.322 & 1.565 \end{bmatrix} \cdot 10^9 \qquad M = \begin{bmatrix} 0.24 & 0 & 0 & 0 \\ 0 & 1.16 & 0 & 0 \\ 0 & 0 & 0.24 & 0 \\ 0 & 0 & 0 & 0.68 \end{bmatrix} \cdot 10^6 \tag{20}$$

Rayleigh proportional damping, $C = \alpha_0 M + \alpha_1 K$, is assumed with estimated proportionality constants $\alpha_0 = 0.24$ and $\alpha_1 = 0.002$, which provide $\xi_1 = 3\%$ and $\xi_3 = 4\%$ critical damping for the first and the third modes, respectively. Calculated modal frequencies and equivalent damping ratios for all modes are shown in Table 1

Initial modal parameter identification

The initial modal parameter identification is carried out assuming no a priori knowledge about the structure is known. The identification is implemented assuming the input ground excitation is not known (output only method). Thus, the objective function is formulated using Equation (13).

Two different input ground motions are selected to simulate the response of a linear structure: a) 2 minute long broadband 2.5%g RMS white noise excitation with constant frequency distribution; and b) Landers 1992 earthquake excitation with peak ground acceleration (PGA) of 0.17g . Time histories of the selected ground input motions are shown in Figure 5. The identification is based on the recorded time series of the whole response (120s for WN and 50s for EQ event). The mass matrix is assumed to be calculated with 30% error, thus $M_{ident} = Z \cdot M$, where the assumed scaling matrix is $Z = diag\left(\begin{bmatrix} 1 & 0.7 & 1.3 & 0.7 \end{bmatrix}\right)$. The effective peak isolation width used in Equation (12) is $W = 5$.

RESULTS AND DISCUSSION

Initial modal parameter identification

Identification based on white noise excitation

The initial modal parameter identification is carried out using 30 of the 120 seconds white noise excitation response data. It is assumed no input ground acceleration is recorded. Thus, identification is based only on the measured acceleration response data. Identification is carried out for 3 different RMS added signal noise levels (0%, 5% and 20%) where the RMS noise is a random normal distribution of the square root of the average of the clean (no noise) simulated measurement with 99.7% of random values within the defined noise level. Identification results are shown in Tables 2 to 4.

The identified modal frequencies presented in Table 2 demonstrate very good agreement for all the noise levels and the discrepancies, Δf, are lower than 1%. The identified equivalent modal damping ratios, presented Table 3 demonstrate poorer consistency compared to identified modal frequencies. The maximum captured error is $\Delta\xi_1 = 16.3\%$, for the largest 20% RMS noise. Large discrepancies can be associated to the relatively short 30 seconds window chosen and low sensitivity of the damping ratio with respect to least squares cost function.

Table 4 shows the identified mode shape coefficients , $\hat{\phi}$. The method yields accurate mode shape coefficient identification even for high signal noise levels. The maximum captured relative error is $\Delta\xi = 4.52\%$, for the 20% added RMS noise case.

Identification based on earthquake excitation

Initial modal parameter identification based on the earthquake response is carried out using 50 seconds of recorded absolute acceleration response data. It is assumed no input ground acceleration is recorded. Thus, identification is based only on the measured response data. As for the white noise excitation data, the identification is carried out for 3 different added signal noise levels. The identified modal frequencies shown in Table 5 demonstrate very good agreement for all the noise levels and the discrepancies, Δf, are lower than 1%.

The identified equivalent damping ratios, $\hat{\xi}$, shown in Table 6, demonstrate smaller errors compared to identification results based on WN excitation. More accurate values can be explained by the longer analysed response time history used for identification. The maximum recorded relative error is $\Delta\xi = 7.0\%$ corresponding to 20% added RMS noise.

Table 7 shows the identified mode shape coefficients , $\hat{\phi}$. The method yields accurate mode shape coefficient identification for all the noise levels. The maximum captured relative error is $\Delta\phi = 6.85\%$, for the 5% signal noise levels.

The results show the proposed method is capable of accurate identification of modal parameters. The initial parameter identification for a 4 DOF system is carried out using only the measured response assuming the system is time-invariant. The identified modal frequencies and mode shape coefficients demonstrate very good consistency with the simulated model for all the noise levels. In contrast, identification of the equivalent modal damping ratios tend to yield lower accuracy. Similar findings have been obtained in a number of studies (Luş et al. 2002; Moaveni et al. 2010; Hong et al. 2009), where the identified damping ratios demonstrated larger deviations than the frequencies. The method yields equally accurate identification for both white noise and earthquake induced ground motion, again, assuming the input is unknown and using output only method.

Limitations

The proposed method operates in the modal space and is based on mode decomposition. Thus a linear time-invariant system (LTI) is assumed throughout the analyzed time window. However, strong ground motions can trigger inelastic behaviour, meaning the principle of mode superposition will no longer be valid. However, most of structures exhibit non-linear behaviour only for a very short time period and the non-linear part comprises a relatively small part of the time history response. In such cases, the method can be applied to shorter time windows, meaning the time windows containing inelastic structural response will be approximated by average mode shape coefficient values providing the best mode decoupling. Tracking their evolution over time can provide a good measure of non-linear monitoring.

The method also requires user judgement, especially in situations where the signal noise appears in the form of poles in the frequency spectrum. These poles might falsely be misinterpreted as modal poles, thus yielding incorrect identification results. However, the results presented here show excellent robustness to white noise and accuracy for ambient or more common smaller seismic inputs, which are the dominant events seen.

User input is also important to prevent error propagation as the identification is carried out sequentially. Poor modal parameter identification might affect the identification of the other modes. The main pivot point of the method is solving the unconstrained optimization problem. Therefore, there is a risk of solver reaching a local solution instead of global solution. Moreover, optimization might become a difficult task in situations where a large number of DOFs are monitored. It should also be noted that the current method is limited to real-valued modes as it solely relies on modal decomposition.

CONCLUSIONS

This study presents a novel output only modal parameter estimation technique, capable of identifying of modal parameters in brief time windows. The method is based on the principle of mode superposition and assumes that the system is linear time-invariant and the modes are real-valued. The method is an output-only modal parameter identification technique and is thus not limited to any type of input loading. This feature is important, since many other system identification methods rely on assumptions about the input loading, such as that it is broad band white noise. Thus, the approach presented can provide a better insight into structures subjected to strong ground motion events, assuming the structure does not exhibit strong non-linearities.

The method is validated using a simulated data for a 4 DOF time-invariant system, which represents a simplified version of a bridge pier and provides excellent validation since the truth is known. The results show the method is capable of identifying modal parameters within 7% relative error in the presence of 20% RMS noise added.

Finally, the presented general mode identification procedure can be easily implemented into more complex MDOF systems as it does not need to rely on any of physical parameters.

DATA AVAILABILITY STATEMENT

Some or all data, models, or code generated or used during the study are available from the corresponding author by request. The following items can be provided: input earthquake excitation dataset, numerical simulation and system identification codes written in MATALB.

ACKNOWLEDGEMENTS

The scholarship support of the New Zealand Earthquake Commission (EQC) for the first author is greatly acknowledged.

REFERENCES

Allemang, R. J. (2003). "The Modal Assurance Criterion –Twenty Years of Use and Abuse." *SOUND AND VIBRATION*, 1(August), 14–21.

Amezquita-Sanchez, J. P. and Adeli, H. (2015). "Synchrosqueezed wavelet transform-fractality model for locating, detecting, and quantifying damage in smart highrise building structures." *Smart Materials and Structures*, 24(6), 065034.

Astroza, R., Ebrahimian, H., Conte, J., Restrepo, J., and Hutchinson, T. (2013). "Statistical analysis of the identified modal properties of a 5-story RC seismically damaged building specimen." *Safety, Reliability, Risk and Life-Cycle Performance of Structures and Infrastructures - Proceedings of the 11th International Conference on Structural Safety and Reliability, ICOSSAR 2013*, number ii, 4593–4600.

Astroza, R., Ebrahimian, H., Conte, J. P., Restrepo, J. I., and Hutchinson, T. C. (2016a). "Influence of the construction process and nonstructural components on the modal properties of a five-story building." *Earthquake Engineering & Structural Dynamics*, 45(7), 1063–1084.

Astroza, R., Ebrahimian, H., Conte, J. P., Restrepo, J. I., and Hutchinson, T. C. (2016b). "System identification of a full-scale five-story reinforced concrete building tested on the NEES-UCSD shake table." *Structural Control and Health Monitoring*, 23(3), 535–559.

Astroza, R., Ebrahimian, H., Conte, J. P., Restrepo, J. I., and Hutchinson, T. C. (2016c). "System identification of a full-scale five-story reinforced concrete building tested on the NEES-UCSD shake table." *Structural Control and Health Monitoring*, 23(3), 535–559.

Bodeux, J. B. and Golinval, J. C. (2001). "Application of ARMAV models to the identification and damage detection of mechanical and civil engineering structures." *Smart Materials and Structures*, 10(3), 479–489.

Brincker, R., Ventura, C., and Andersen, P. (2001). "Damping estimation by frequency domain decomposition." *19th International Modal Analysis Conference*, 698–703.

Brownjohn, J. M., Magalhaes, F., Caetano, E., and Cunha, A. (2010). "Ambient vibration re-testing and operational modal analysis of the Humber Bridge." *Engineering Structures*, 32(8), 2003–2018.

Caicedo, J. M. (2011). "Practical guidelines for the natural excitation technique (NExT) and the eigensystem realization algorithm (ERA) for modal identification using ambient vibration." *Experimental Techniques*, 35(August), 52–58.

Carden, E. and Brownjohn, J. M. (2008). "ARMA modelled time-series classification for structural health monitoring of civil infrastructure." *Mechanical Systems and Signal Processing*, 22(2), 295–314.

CEN (2004). "Eurocode 8: Design of structures for earthquake resistance." 120, 1–229.

Chopra, A. K. (1995). *Dynamics of structures : theory and applications to earthquake engineering*. Prentice Hall.

da Silva, S., Dias Júnior, M., Lopes Junior, V., and Brennan, M. J. (2008). "Structural damage detection by fuzzy clustering." *Mechanical Systems and Signal Processing*, 22(7), 1636–1649.

Doebling, S., Farrar, C., Prime, M., and Shevitz, D. (1996). "Damage identification and health monitoring of structural and mechanical systems from changes in their vibration characteristics: A literature review." *The Shock and Vibration Digest*, LA–13070-(August 2016), 127.

Ewins, D. J. (2000). *Modal testing : theory, practice, and application*. Research Studies Press.

Farrar, C. R., Doebling, S. W., Cornwell, P. J., and Straser, E. G. (1996). "Variability of modal parameters measured on the Alamosa Canyon Bridge." *Report no.*, Los Alamos National Lab., NM (United States).

Fraraccio, G., Brügger, A., and Betti, R. (2008). "Identification and Damage Detection in Structures Subjected to Base Excitation." *Experimental Mechanics*, 48(4), 521–528.

Hong, A. L., Betti, R., and Lin, C.-C. (2009). "Identification of dynamic models of a building structure using multiple earthquake records." *Structural Control and Health Monitoring*, 16(2), 178–199.

Jacobsen, N.-J., Andersen, P., and Brincker, R. (2008). "Applications of frequency domain curve-fitting in the EFDD technique." *Proceedings IMAC XXVI Conference*.

Juang, J.-N. and Pappa, R. S. (1985). "Eigensystem realization algorithm for modal parameter identification and model reduction." *Journal of Guidance, Control, and Dynamics*, 8(5), 620 – 627.

Juang, J.-N., Phan, M., Horta, L. G., and Longman, R. W. (1993). "Identification of observer/Kalman filter Markov parameters: theory and experiments." *Journal of Guidance, Control, and Dynamics*, 16(2), 320–329.

Luş, H., Betti, R., and Longman, R. W. (2002). "Obtaining refined first-order predictive models of linear structural systems." *Earthquake Engineering and Structural Dynamics*, 31(7), 1413–1440.

Luş, H., Betti, R., Yu, J., and De Angelis, M. (2004). "Investigation of a System Identification Methodology in the Context of the ASCE Benchmark Problem." *Journal of Engineering Mechanics*, 130(January), 71–84.

Moaveni, B., He, X., Conte, J., and de Callafon, R. (2008). "Damage identification of a composite beam using finite element model updating." *Computer-Aided Civil and Infrastructure Engineering*, 23(5), 339 – 359.

Moaveni, B., He, X., Conte, J. P., and Restrepo, J. I. (2010). "Damage identification study of a seven-story full-scale building slice tested on the UCSD-NEES shake table." *Structural Safety*, 32(5), 347–356.

Moaveni, B., Stavridis, A., Lombaert, G., and Conte, J. P. (2013). "Finite-Element Model Updating for Assessment of Progressive Damage in a 3-Story Infilled RC Frame." *Journal of Structural Engineering*, 139(10).

Moncayo, H., Marulanda, J., and Thomson, P. (2010). "Identification and Monitoring of Modal Parameters in Aircraft Structures Using the Natural Excitation Technique (NExT) Combined with the Eigensystem Realization Algorithm (ERA)." *Journal of Aerospace Engineering*, 23(2), 99–104.

Nagarajaiah, S. and Basu, B. (2009). "Output only modal identification and structural damage detection using time frequency & wavelet techniques." *Earthquake Engineering and Engineering Vibration*, 8(4), 583–605.

Pappa, R. S., James, G. H., and Zimmerman, D. C. (1998). "Autonomous Modal Identification of the Space Shuttle Tail Rudder." *Journal of Spacecraft and Rockets*, 35(2), 163–169.

Ren, W.-X. and De Roeck, G. (2002). "Structural damage identification using modal data. II: Test verification." *Journal of Structural Engineering*, 128(1), 96–104.

Saaed, T. E. and Nikolakopoulos, G. (2016). "Identification of building damage using ARMAX model: a parametric study." *Diagnostyka*, 17.

Schoettler, M. J., Restrepo, J., Guerrini, G., Duck, D. E., and Carrea, F. (2012). "A Full-Scale, Single-Column Bridge Bent Tested by Shake-Table Excitation." *Report No. August*, PEER Report No. 2015/02, Department of Civil Engineering,University of Nevada.

Singhal, A. and Kiremidjian, A. S. (1996). "Method for probabilistic evaluation of seismic structural damage." *Journal of Structural Engineering*, 122(12), 1459–1467.

Sohn, H. and Farrar, C. R. (2001). "Damage diagnosis using time series analysis of vibration signals." *Engineering Analysis*, 10(3), 446–451.

Vicario, F., Phan, M. Q., Betti, R., and Longman, R. W. (2015). "Output-only observer/Kalman filter identification (O3KID)." *Structural Control and Health Monitoring*, 22(5), 847–872.

Zhou, C., Chase, J. G., Rodgers, G. W., Tomlinson, H., and Xu, C. (2015). "Physical parameter identification of structural systems with hysteretic pinching." *Computer-Aided Civil and Infrastructure Engineering*, 30(4), 247–262.

Zhou, C., Chase, J. G., Rodgers, G. W., and Xu, C. (2017). "Comparing model-based adaptive LMS filters and a model-free hysteresis loop analysis method for structural health monitoring." *Mechanical Systems and Signal Processing*, 84, 384–398.

List of Tables

TABLE 1. Calculated modal parameters of a 4 DOF system

Mode	1	2	3	4
Modal frequency, f (Hz)	1.39	1.45	6.46	8.1
Modal damping, ξ(%)	3.00	2.94	4.00	4.80

TABLE 2. Identified modal frequencies for different signal noise levels

Mode	f_{model}, Hz	$\hat{f}_{id,0}, Hz$	Δf, %	$\hat{f}_{id,5\%}, Hz$	Δf, %	$\hat{f}_{id,20\%}, Hz$	Δf, %
Mode 1	1.392	1.396	0.29	1.396	0.27	1.394	0.14
Mode 2	1.449	1.459	0.68	1.459	0.68	1.459	0.67
Mode 3	6.457	6.440	-0.27	6.439	-0.29	6.448	-0.14
Mode 4	8.103	8.074	-0.36	8.074	-0.37	8.061	-0.52

TABLE 3. Identified equivalent modal damping for different signal noise levels

Mode	ξ_{model}	$\hat{\xi}_{id,0}$	$\Delta\xi$, %	$\hat{\xi}_{id,5\%}$	$\Delta\xi$, %	$\hat{\xi}_{id,20\%}$	$\Delta\xi$, %
Mode 1	0.030	0.035	15.7	0.034	14.3	0.035	16.33
Mode 2	0.029	0.026	-10.2	0.026	-10.2	0.026	-10.88
Mode 3	0.040	0.042	6.0	0.042	5.7	0.041	3.25
Mode 4	0.048	0.049	1.7	0.049	1.5	0.049	2.08

TABLE 4. Identified mode shape coefficients for different levels of signal noise

Mode		ϕ_{model}	$\hat{\phi}_{id,0}$	$\Delta\phi$, %	$\hat{\phi}_{id,5\%}$	$\Delta\phi$, %	$\hat{\phi}_{id,20\%}$	$\Delta\phi$, %
Mode 1	$\hat{\phi}_{1,1}$	1.00	1.00	0.00	1.00	0.00	1.00	0.00
	$\hat{\phi}_{2,1}$	-0.22	-0.22	2.62	-0.23	3.31	-0.22	2.02
	$\hat{\phi}_{3,1}$	0.00	0.00	-0.33	0.00	-0.35	0.00	-0.34
	$\hat{\phi}_{4,1}$	0.00	0.01	1.03	0.01	1.06	0.01	1.04
Mode 2	$\hat{\phi}_{1,2}$	0.00	0.01	0.60	0.01	0.61	0.01	0.58
	$\hat{\phi}_{2,2}$	0.00	0.01	0.80	0.01	0.80	0.01	0.77
	$\hat{\phi}_{3,2}$	1.00	1.00	0.00	1.00	0.00	1.00	0.00
	$\hat{\phi}_{4,2}$	0.21	0.21	-0.14	0.21	-0.09	0.21	0.00
Mode 3	$\hat{\phi}_{1,3}$	1.00	1.00	0.00	1.00	0.00	1.00	0.00
	$\hat{\phi}_{2,3}$	0.93	0.93	-0.44	0.93	-0.57	0.92	-1.08
	$\hat{\phi}_{3,3}$	0.00	0.02	2.11	0.02	1.99	0.02	2.42
	$\hat{\phi}_{4,3}$	0.00	-0.04	-4.44	-0.04	-4.45	-0.05	-4.52
Mode 4	$\hat{\phi}_{1,4}$	0.00	0.00	-0.09	0.00	-0.13	0.00	0.02
	$\hat{\phi}_{2,4}$	0.00	0.00	0.03	0.00	0.04	0.00	0.00
	$\hat{\phi}_{3,4}$	-0.61	-0.62	0.23	-0.62	0.41	-0.61	-0.65
	$\hat{\phi}_{4,4}$	1.00	1.00	0.00	1.00	0.00	1.00	0.00

TABLE 5. Identified modal frequencies for different signal noise levels based on earthquake response data

Mode	f_{model}, Hz	$\hat{f}_{id,0}, Hz$	$\Delta f, \%$	$\hat{f}_{id,5\%}, Hz$	$\Delta f, \%$	$\hat{f}_{id,20\%}, Hz$	$\Delta f, \%$
Mode 1	1.392	1.397	0.32	1.396	0.31	1.397	0.34
Mode 2	1.449	1.451	0.11	1.451	0.11	1.451	0.12
Mode 3	6.457	6.433	-0.37	6.434	-0.37	6.435	-0.35
Mode 4	8.103	8.032	-0.88	8.033	-0.87	8.033	-0.87

TABLE 6. Equivalent modal damping for different signal noise levels identified from response to earthquake excitation

Mode	ξ_{model}	$\hat{\xi}_{id,0}$	$\Delta\xi$, %	$\hat{\xi}_{id,5\%}$	$\Delta\xi$, %	$\hat{\xi}_{id,20\%}$	$\Delta\xi$, %
Mode 1	0.030	0.028	-6.7	0.028	-7.0	0.028	-7.00
Mode 2	0.029	0.028	-3.4	0.028	-3.7	0.028	-3.40
Mode 3	0.040	0.039	-1.8	0.039	-1.8	0.039	-1.75
Mode 4	0.048	0.046	-4.6	0.046	-5.0	0.046	-4.79

TABLE 7. Identified mode shape coefficients for different levels of signal noise based on the response to earthquake excitation

Mode		ϕ_{model}	$\hat{\phi}_{id,0}$	$\Delta\phi$, %	$\hat{\phi}_{id,5\%}$	$\Delta\phi$, %	$\hat{\phi}_{id,20\%}$	$\Delta\phi$, %
Mode 1	$\hat{\phi}_{1,1}$	1.00	1.00	0.00	1.00	0.00	1.00	0.00
	$\hat{\phi}_{2,1}$	-0.22	-0.21	-2.07	-0.21	-1.88	-0.21	-2.25
	$\hat{\phi}_{3,1}$	0.00	0.00	-0.04	0.00	-0.03	0.00	-0.03
	$\hat{\phi}_{4,1}$	0.00	0.00	0.13	0.00	0.11	0.00	0.09
Mode 2	$\hat{\phi}_{1,2}$	0.00	0.00	0.05	0.00	0.08	0.00	0.07
	$\hat{\phi}_{2,2}$	0.00	0.00	0.07	0.00	0.11	0.00	0.09
	$\hat{\phi}_{3,2}$	1.00	1.00	0.00	1.00	0.00	1.00	0.00
	$\hat{\phi}_{4,2}$	0.21	0.20	-4.13	0.20	-4.17	0.20	-4.13
Mode 3	$\hat{\phi}_{1,3}$	1.00	1.00	0.00	1.00	0.00	1.00	0.00
	$\hat{\phi}_{2,3}$	0.93	0.93	-0.10	0.93	0.04	0.94	0.58
	$\hat{\phi}_{3,3}$	0.00	0.05	4.50	0.05	4.53	0.04	3.89
	$\hat{\phi}_{4,3}$	0.00	-0.07	-6.79	-0.07	-6.85	-0.07	-6.83
Mode 4	$\hat{\phi}_{1,4}$	0.00	0.00	-0.15	0.00	-0.17	0.00	-0.01
	$\hat{\phi}_{2,4}$	0.00	0.00	0.05	0.00	0.06	0.00	0.00
	$\hat{\phi}_{3,4}$	-0.61	-0.62	0.39	-0.61	-0.21	-0.61	0.10
	$\hat{\phi}_{4,4}$	1.00	1.00	0.00	1.00	0.00	1.00	0.00

List of Figures

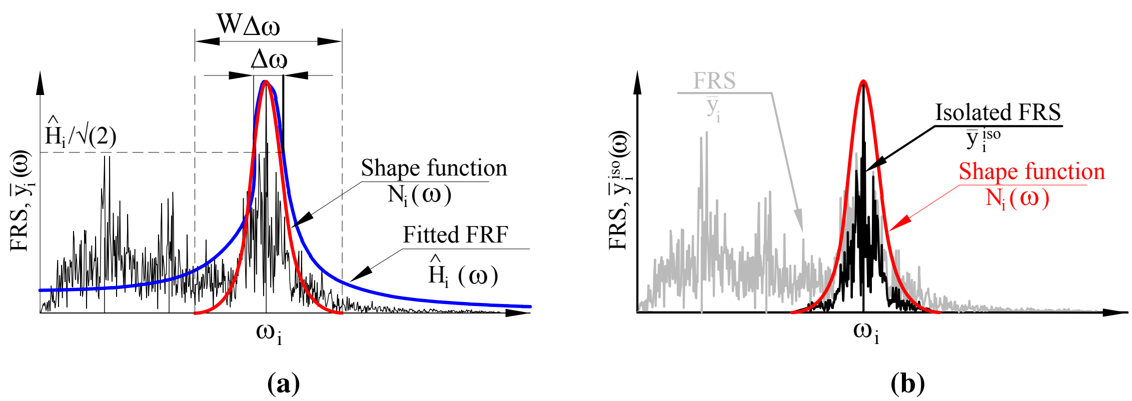

Fig. 1. (a) FRF fitting, frequency bandwidth and shape function estimation (b) Shape function, N_i, overlapped with i^{th} mode FRS, $\overline{y}_i(\omega)$, to obtain isolated FRS, $\overline{y}_i^{iso}$

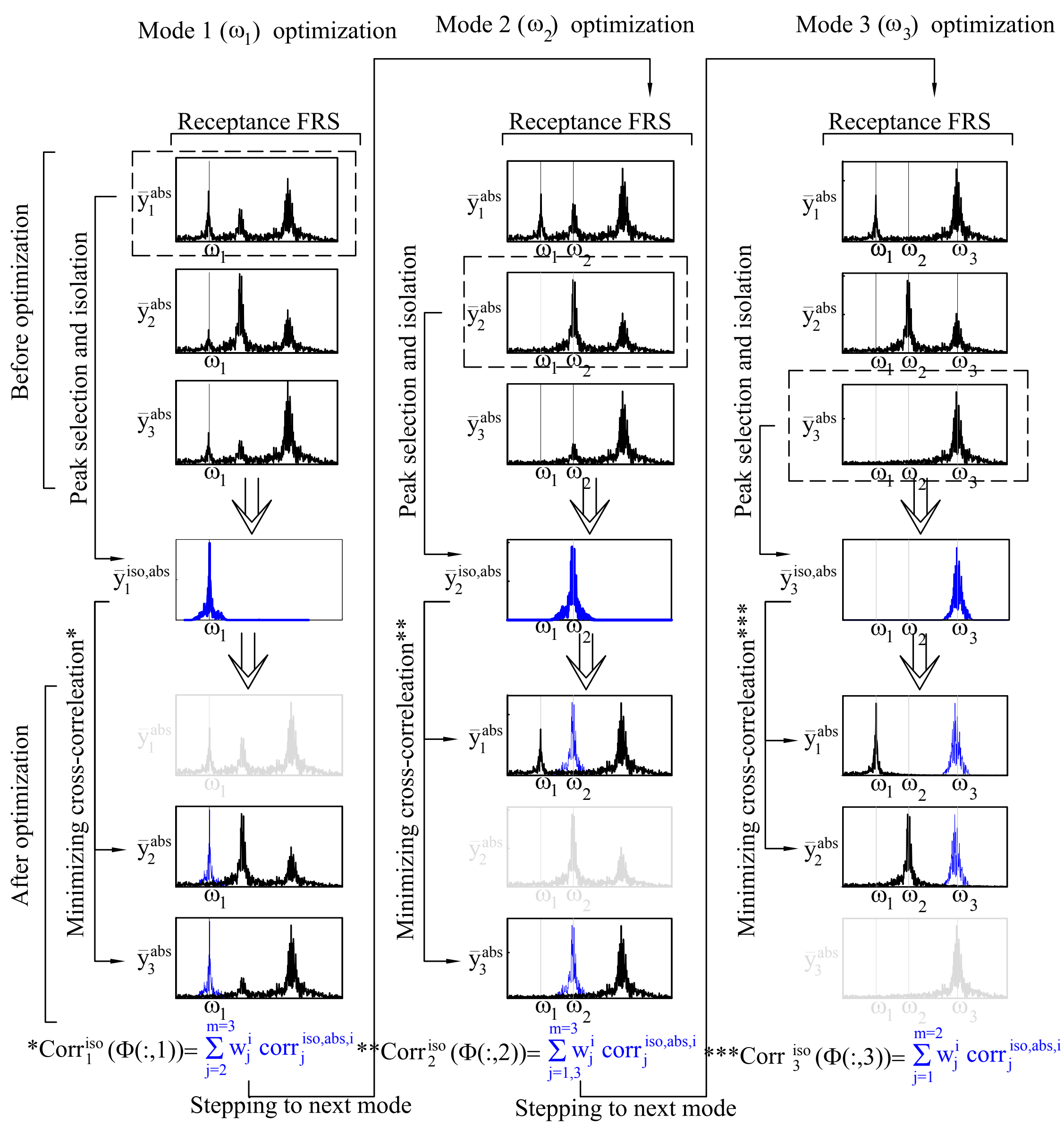

Fig. 2. Mode-by-mode optimization example for a 3 DOF system. The term *abs* in the subscript of $corr_j^{iso,abs,i}$ and $\bar{y}_i^{abs}$ refers to the calculations based on the absolute measurements.

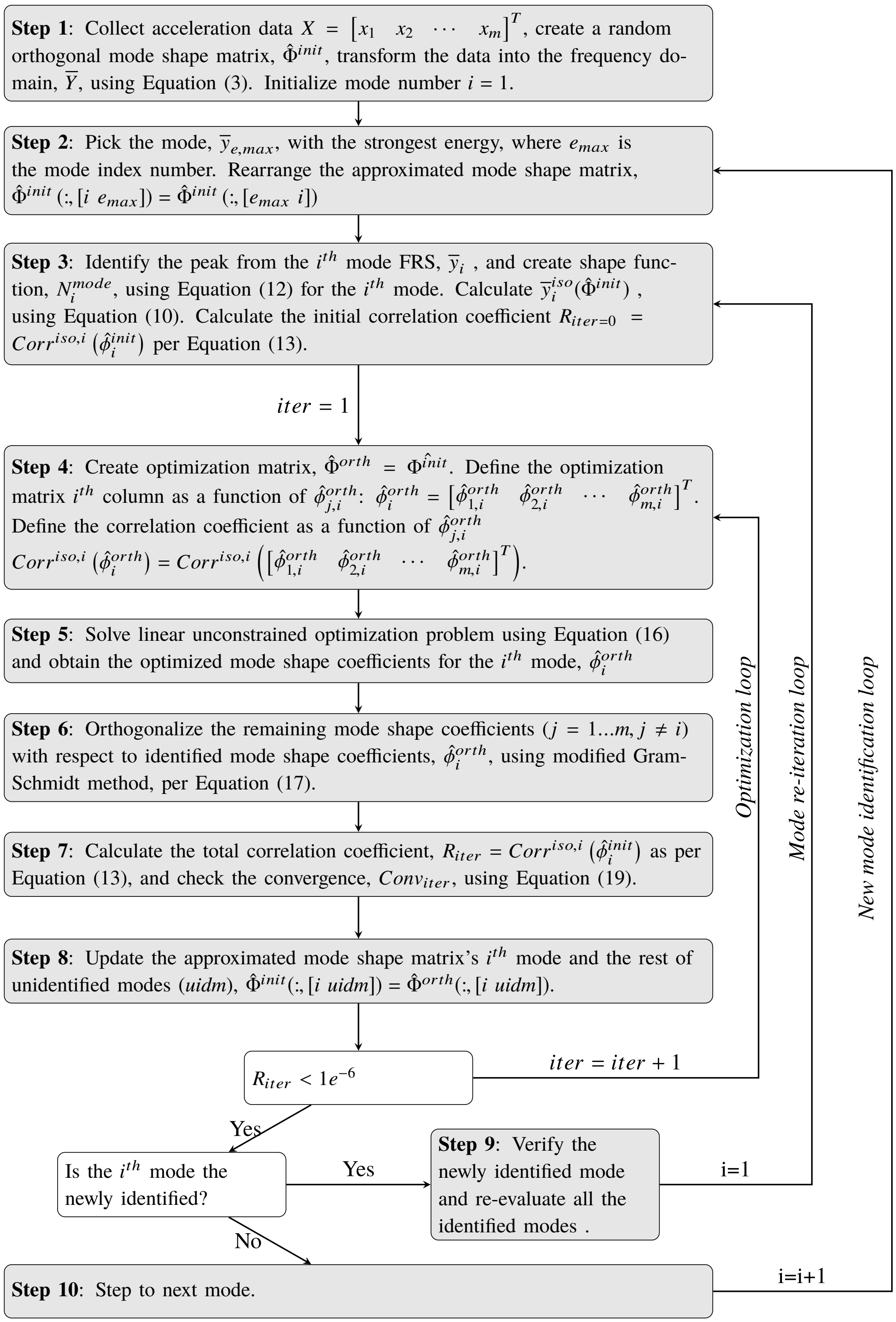

Fig. 3. Flow chart for initial mode-by-mode optimization for any given time window

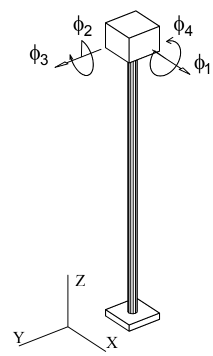

Fig. 4. A simplified 4 DOF model of a bridge pier test structure

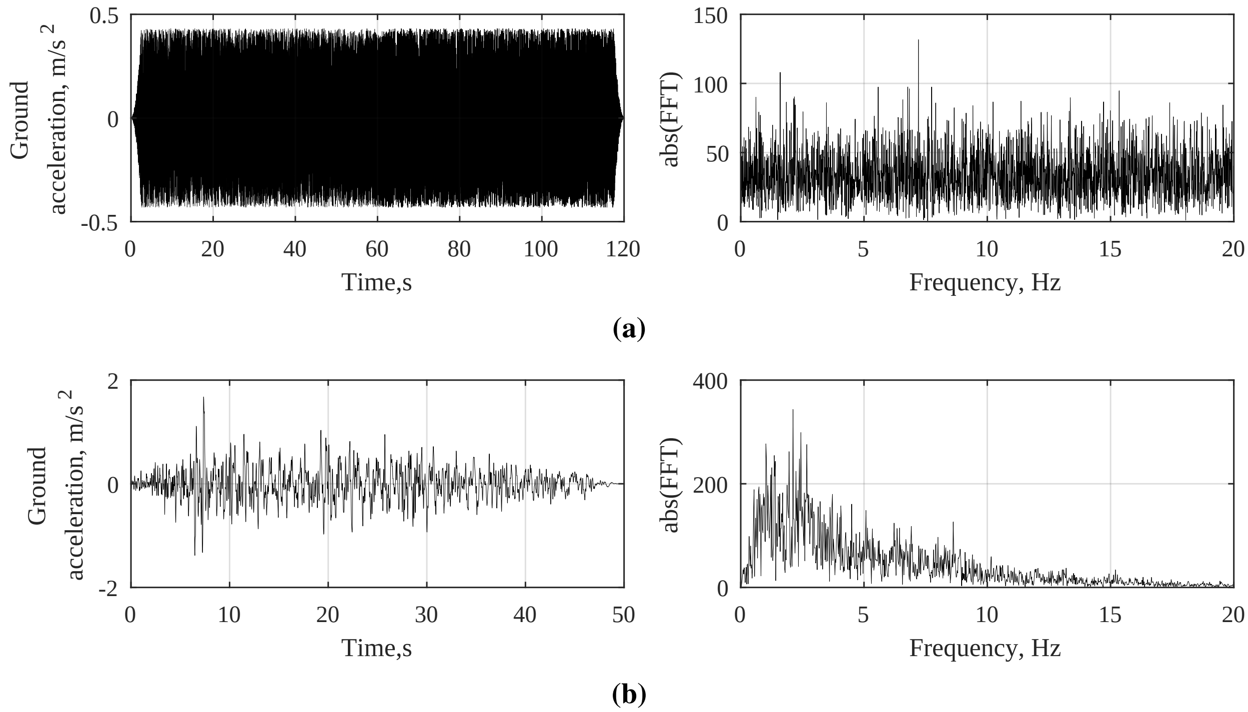

Fig. 5. Input ground motion time histories and frequency spectra for (a) white noise 2.5%g RMS and (b) selected earthquake ground motions

Figure 1a

Click here to access/download;Figure;Figure1a_FRS.pdf

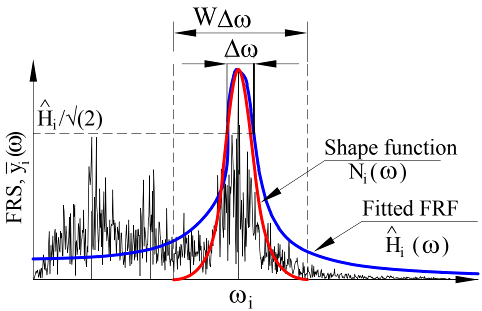

Figure 1b

Click here to access/download;Figure;Figure1b_PeakIsol

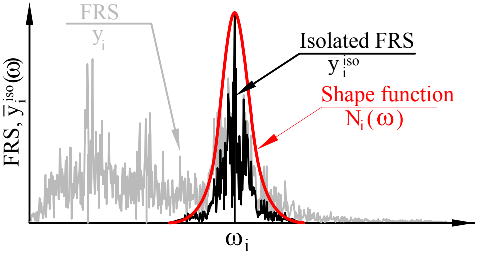

Figure 2

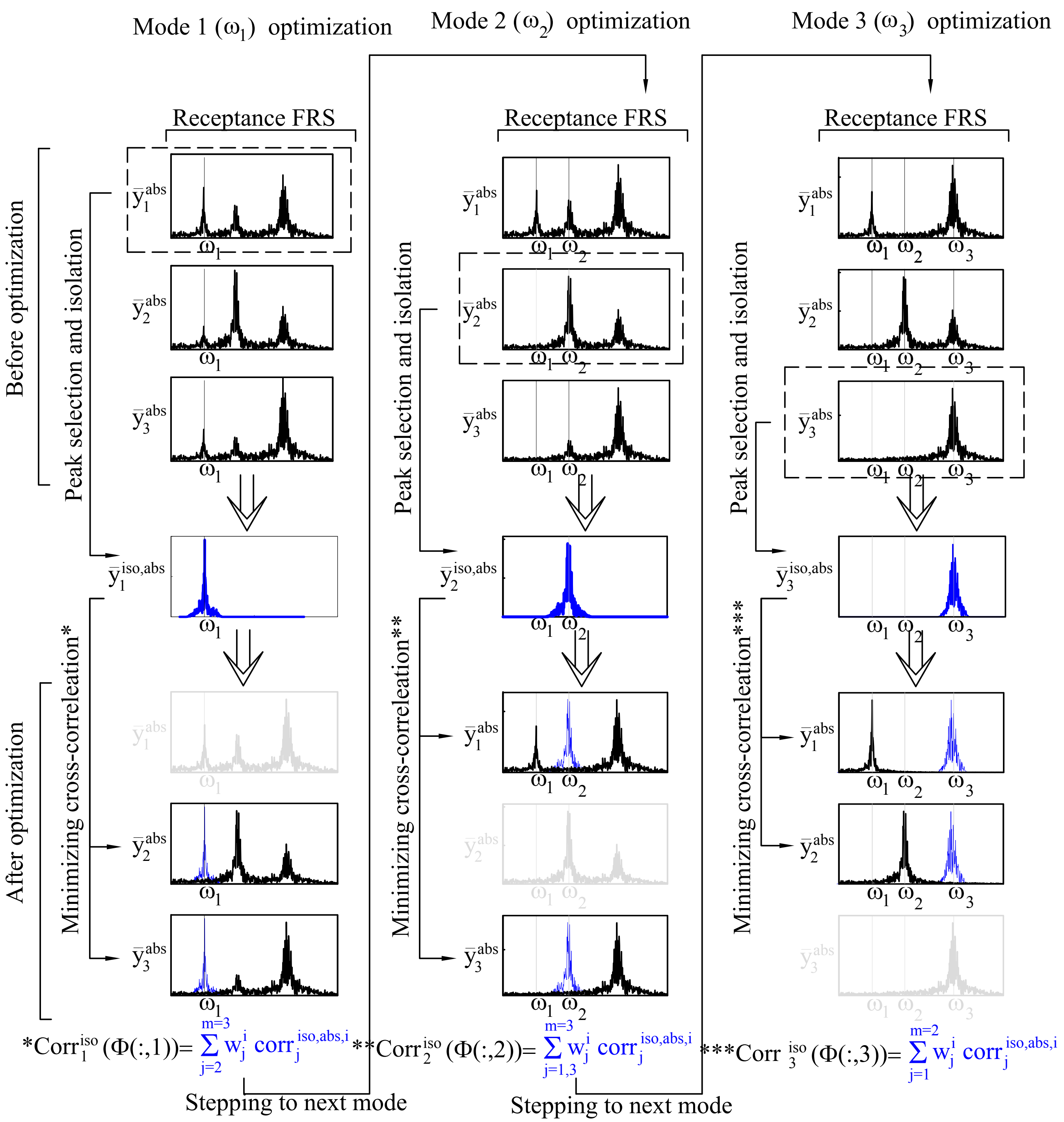
Mode 1 (ω1) optimization
Mode 2 (ω2) optimization
Mode 3 (ω3) optimization
Receptance FRS
Receptance FRS
Receptance FRS
Before optimization
After optimization
Peak selection and isolation
Minimizing cross-correleation*
Minimizing cross-correleation**
Minimizing cross-correleation***
ȳ1abs
ȳ2abs
ȳ3abs
ȳ1iso,abs
ȳ2iso,abs
ȳ3iso,abs
ω1 ω2 ω3
*Corr1iso (Φ(:,1))= Σ j=2 m=3 wji corrjiso,abs,i
**Corr2iso (Φ(:,2))= Σ j=1,3 m=3 wji corrjiso,abs,i
***Corr 3iso (Φ(:,3))= Σ j=1 m=2 wji corrjiso,abs,i
Stepping to next mode
Stepping to next mode

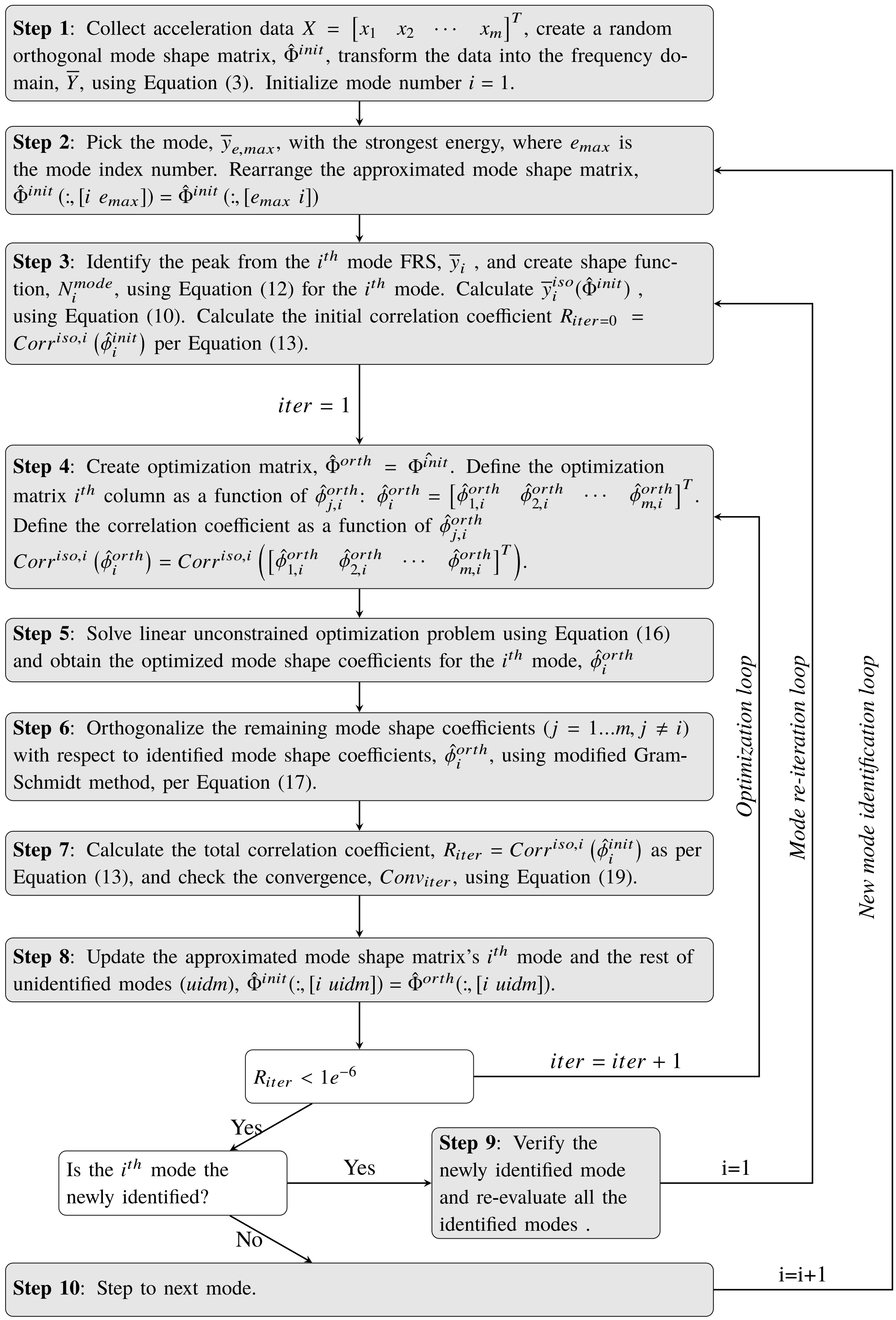
Step 1: Collect acceleration data $X = \begin{bmatrix} x_1 & x_2 & \cdots & x_m \end{bmatrix}^T$, create a random orthogonal mode shape matrix, $\hat{\Phi}^{init}$, transform the data into the frequency domain, $\overline{Y}$, using Equation (3). Initialize mode number $i = 1$.
Step 2: Pick the mode, $\overline{y}_{e,max}$, with the strongest energy, where e_{max} is the mode index number. Rearrange the approximated mode shape matrix, $\hat{\Phi}^{init}(:, [i \;\, e_{max}]) = \hat{\Phi}^{init}(:, [e_{max} \;\, i])$
Step 3: Identify the peak from the i^{th} mode FRS, $\overline{y}_i$, and create shape function, N_i^{mode}, using Equation (12) for the i^{th} mode. Calculate $\overline{y}_i^{iso}(\hat{\Phi}^{init})$, using Equation (10). Calculate the initial correlation coefficient $R_{iter=0} = Corr^{iso,i}\left(\hat{\phi}_i^{init}\right)$ per Equation (13).
$iter = 1$
Step 4: Create optimization matrix, $\hat{\Phi}^{orth} = \hat{\Phi^{init}}$. Define the optimization matrix i^{th} column as a function of $\hat{\phi}_{j,i}^{orth}$: $\hat{\phi}_i^{orth} = \begin{bmatrix} \hat{\phi}_{1,i}^{orth} & \hat{\phi}_{2,i}^{orth} & \cdots & \hat{\phi}_{m,i}^{orth} \end{bmatrix}^T$. Define the correlation coefficient as a function of $\hat{\phi}_{j,i}^{orth}$ $Corr^{iso,i}\left(\hat{\phi}_i^{orth}\right) = Corr^{iso,i}\left(\begin{bmatrix} \hat{\phi}_{1,i}^{orth} & \hat{\phi}_{2,i}^{orth} & \cdots & \hat{\phi}_{m,i}^{orth} \end{bmatrix}^T\right)$.
Step 5: Solve linear unconstrained optimization problem using Equation (16) and obtain the optimized mode shape coefficients for the i^{th} mode, $\hat{\phi}_i^{orth}$
Step 6: Orthogonalize the remaining mode shape coefficients ($j = 1...m, j \neq i$) with respect to identified mode shape coefficients, $\hat{\phi}_i^{orth}$, using modified Gram-Schmidt method, per Equation (17).
Step 7: Calculate the total correlation coefficient, $R_{iter} = Corr^{iso,i}\left(\hat{\phi}_i^{init}\right)$ as per Equation (13), and check the convergence, $Conv_{iter}$, using Equation (19).
Step 8: Update the approximated mode shape matrix's i^{th} mode and the rest of unidentified modes ($uidm$), $\hat{\Phi}^{init}(:, [i \;\, uidm]) = \hat{\Phi}^{orth}(:, [i \;\, uidm])$.
$R_{iter} < 1e^{-6}$
$iter = iter + 1$
Yes
Is the i^{th} mode the newly identified?
Yes
Step 9: Verify the newly identified mode and re-evaluate all the identified modes .
i=1
No
Step 10: Step to next mode.
i=i+1
Optimization loop
Mode re-iteration loop
New mode identification loop

Figure 4 Click here to access/download;Figure;Figure4_ModelView.pdf

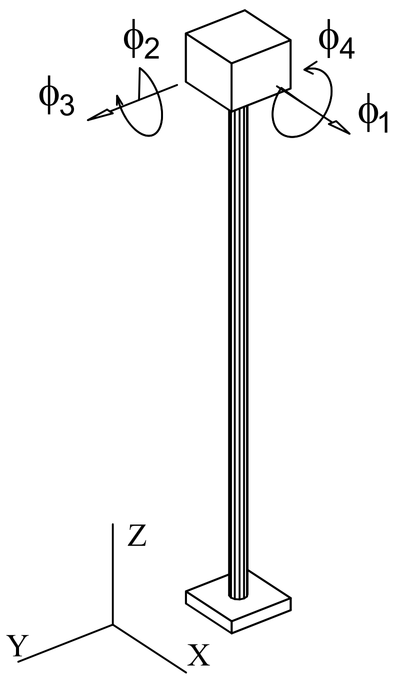

Figure 5a

Click here to access/download;Figure;Figure5a_InputMo

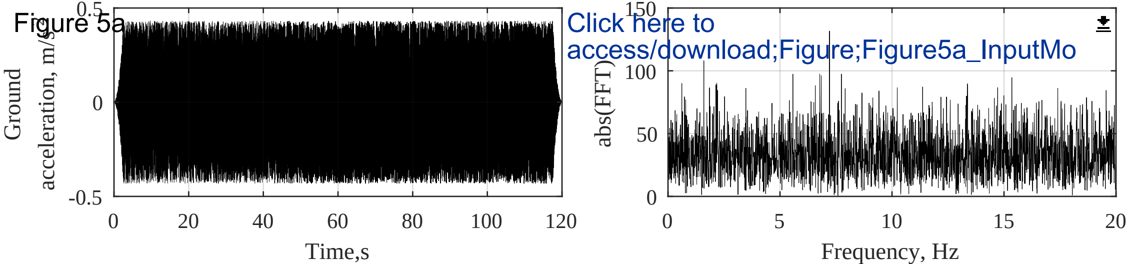

Figure 5b

Click here to access/download;Figure;Figure5b_InputMo